pH-adaptive microlenses using pinned liquid-liquid interfaces actuated by pH-responsive hydrogel

Liang Dong and Hongrui Jiang

Citation: Appl. Phys. Lett. **89**, 211120 (2006); doi: 10.1063/1.2393038
View online: http://dx.doi.org/10.1063/1.2393038
View Table of Contents: http://aip.scitation.org/toc/apl/89/21
Published by the American Institute of Physics

RIGHTSLINK

*p*H-adaptive microlenses using pinned liquid-liquid interfaces actuated by *p*H-responsive hydrogel

Liang Dong and Hongrui Jiang[a)]
Department of Electrical and Computer Engineering, University of Wisconsin-Madison, 1415 Engineering Drive, Madison, Wisconsin 53706

(Received 8 August 2006; accepted 7 October 2006; published online 22 November 2006)

The authors report on variable-focus liquid microlenses self-adaptive to environmental *p*H. The microlens is formed via a water-oil interface stably pinned at a hydrophobic-hydrophilic contact line along an aperture in a flexible slip. A set of hydrogel microposts is photopatterned in a microfluidic chamber around the aperture; the microposts autonomously respond to the environmental *p*H variation by expanding or contracting, thus deforming the aperture slip and tuning the curvature of the water-oil interface and the focal length of the microlens. A single microlens has a tunable focal length from −7.6 mm to −∞ (divergent) and from 8.5 mm to +∞ (convergent). © *2006 American Institute of physics*. [DOI: 10.1063/1.2393038]

The need for variable-focus microlenses coexists with continuing miniaturization trends across various fields, especially in optical imaging, medical diagnostics, and laboratory on a chip.[1–3] Typical variable-focus microlenses are achieved by either changing the refractive index of lens material or the shape of elastomer and liquid droplet.[4–8] Adaptive variable-focus microlenses have also been reported.[9–11] Despite these progresses, there remains a significant need for materials and/or designs of microlenses that exhibit wide tuning range of focal length and do not require complicated external control, especially for applications in bio-optic microfluidic and laboratory-on-a-chip system.

We recently reported smart liquid microlenses inspired by human eye.[12,13] In that concept, an enclosed elastic polymer ring made of stimuli-responsive hydrogel[14] can behave analogous to ciliary muscles of human eye to regulate the shape of a pinned liquid-liquid interface (at the scale of tens to thousands of micrometers, surface tension of liquid plays a dominant role in liquid behavior over gravity[15]). Thus, the focal length of the liquid microlens (i.e., the liquid-liquid interface) is tuned. The ability to convert chemical energy into mechanical energy allows hydrogels to function as autonomous modules to both sense a localized environment (e.g., *p*H, light, temperature, electric fields, and antigen) and accordingly actuate the liquid microlens without using any additional sensor to form a closed-loop feedback. The concept was implemented by harnessing the horizontal expansion and contraction of the hydrogel ring that separated lens liquid from buffer solution (carrying stimuli information) in microfluidic channel. In this letter, we report on another scheme to implement the concept to realize a variable-focus liquid microlens self-adaptive to its local environmental *p*H. The lens device takes advantage of the vertical expansion and contraction of multiple hydrogel microposts that are exposed to the buffer solution (i.e., the lens liquid). This scheme can diversify the lens design to meet specific needs and is potentially beneficial for fast response time and mechanical robustness of the liquid microlens. To demonstrate the self-adaptive functionality, the hydrogel used here is acrylic acid (AA)-based *p*H-responsive hydrogel,[16] which expands in basic solutions and contracts in acidic solutions with a critical volume transition point of *p*H 5.5.

The structure and mechanism of the self-adaptive liquid microlens is described in Fig. 1. A set of microposts made of *p*H-responsive hydrogel is constructed in the microfluidic chamber. A circular aperture is formed in a flexible polymer slip. The sidewall and top side of the aperture are treated as hydrophilic and hydrophobic, respectively. Since aqueous so-

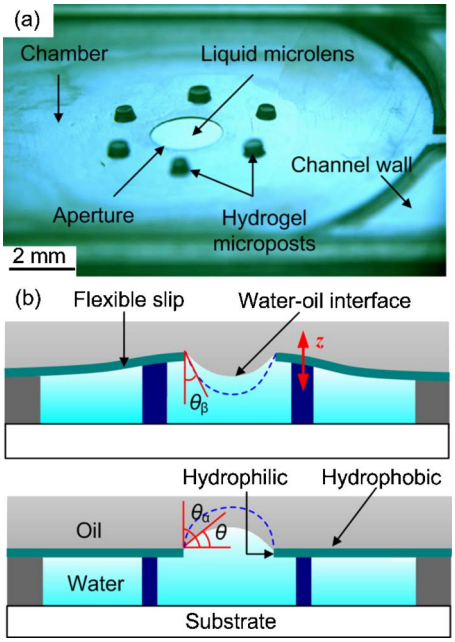

FIG. 1. (Color online) Structure and mechanism of a liquid microlens self-adaptive to environmental *p*H. (a) Optical image of a fabricated device. (b) A microlens is formed via an interface between oil and aqueous solution. The interface is pinned stably at a hydrophobic-hydrophilic contact line along a circular aperture. The liquid meniscus is confined to the aperture. The volume changes of hydrogel microposts cause a flexible aperture slip to bend in the *z* direction. The pinned water-oil interface is pressed downward and upward, thus tuning the focal length of the microlens. Because the refractive index of mineral oil (1.46–1.48) is larger than that of water (1.33–1.34), the microlens protruding upward diverges light, while the one protruding downward converges light. The blue lines represent the critical water-oil interfaces determined by the water contact angles θ_α on the hydrophilic sidewall and θ_β on the hydrophobic top-side surface, respectively.

a)Author to whom correspondence should be addressed; electronic mail: hongrui@engr.wisc.edu

RIGHTSLINK
 © 2006 American Institute of physics

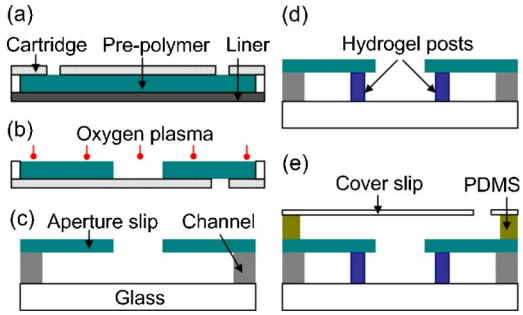

FIG. 2. (Color online) Fabrication process of the liquid microlens.

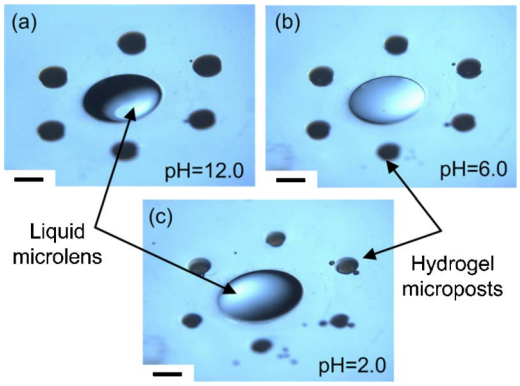

FIG. 3. (Color online) Shapes of liquid microlenses when varying *p*H. Initially the hydrogel microposts are at expanded state (*p*H=12.0), pushing against the substrate to bend the aperture slip upward, and the liquid meniscus protrudes downward. As low *p*H buffers flow into the microfluidic chamber, the hydrogel microposts contract, and the flexible slip bends back to press the liquid meniscus to bulge upward. Scale bars are 1 mm.

lutions remain only on hydrophilic pathways at pressures below a critical value, part of the water-based liquid attached to the sidewall can form a liquid meniscus protruding downward at low pressure and upward at high pressure. The water-based liquid containing stimuli acts as lens liquid, flowing in the chamber; oil is used to prevent the evaporation; and the liquid microlens is naturally formed through the pinned water-oil interface. As illustrated in Fig. 1(b), when exposed to a changing *p*H environment, the hydrogel microposts can expand to bend a flexible aperture slip up or recover the slip at the contracted state. Correspondingly, the liquid meniscus can bow downward or be pressed to bulge out of the aperture. The shape of the microlens is changed in terms of angle θ; therefore the focal length of the microlens is tuned.

The microlens can transform from convergent to divergent by varying the pressure difference across the water-oil interface. The maximum angles $\theta_{1,2}$ for divergent and convergent microlenses are set by the water contact angles θ_α on the sidewall and θ_β on the top-side surface, respectively. Two critical pressure differences $P_{1,2}$ at $\theta_1=\theta_\alpha$ and $\theta_2=-(90°-\theta_\beta)$, respectively, are calculated using the Young-Laplace equation $P=\gamma(1/R_1+1/R_2)$, where P, γ, and $R_{1,2}$ are the pressure difference across the curved interface, the liquid surface free energy, and the radii of the curved interface, respectively. For a circular aperture, $R_1=R_2=R=r/\sin\theta$, where r is the radius of the aperture. For $r=500$ μm, P_1 and P_2 are 416 and -530 N/m^2, respectively. The negative pressure difference represents that the pressure at the water side is less than that at the oil side.

The device is fabricated by utilizing liquid-phase photopolymerization[17] (LP^3) without the need for a clean room facility (Fig. 2). The fabrication starts with a polycarbonate cartridge (HybriWells, Grace Bio-Labs, Bend, OR) filled with isobornyl acrylate-based prepolymer [poly(IBA)] mixture.[12] A circular aperture is formed inside the cartridge via direct photopatterning of the mixture (UV intensity $I_{\mathrm{UV,poly(IBA)}}=7.7$ mW/cm^2, exposure time $t_{\mathrm{UV,poly(IBA)}}=24$ s) [Fig. 2(a)]. After peeling off the thin liner of the cartridge, 100% ethanol is used to remove the unpolymerized prepolymer. To make the poly(IBA) sidewall of the circular aperture hydrophilic, an oxygen plasma treatment is carried out using a reactive ion etching system [Technics Micro-RIE series 800-IIC, power supply of 70 W at 13.56 MHz, oxygen flow rate of 3.0 SCCM (SCCM denotes cubic centimeters per minute at STP); gas pressure of 107 mTorr, and treatment time of 40 s] [Fig. 2(b)]. Next, the cartridge is removed and a cavity is formed by adhering the poly(IBA) aperture slip to using 500 μm thick double-side adhesive spacer tapes. The poly(IBA) microchannel and hydrogel microposts are constructed inside the cavity by using sequential step-and-repeat LP^3 processes ($I_{\mathrm{UV,poly(IBA)}}=8.5$ mW/cm^2 and $t_{\mathrm{UV,poly(IBA)}}=34.5$ s; $I_{\mathrm{UV,AA}}=10$ mW/cm^2 and $t_{\mathrm{UV,AA}}=45.3$ s) [Figs. 2(c) and 2(d)]. Then, the top-side surface of the aperture slip is rendered hydrophobic by coating it with an octadecyltrichlorosilane solution diluted by hexadecane [0.2% (v/v)]. To store the oil on top of the water, a polydimethylsiloxane (PDMS) elastomer fence, bonded with a glass cover slip, is glued to the aperture slip. An initial liquid meniscus is formed by loading water into the chamber through the input. Initial curvature of the meniscus depends on the amount of the loaded water. Finally, mineral oil is filled into the PDMS fence through a hole drilled on the cover slip. Potentially, the oil can be stored in a separate reservoir to allow the oil movement [Fig. 2(e)].

Typical shapes of the liquid microlens at varying *p*H are demonstrated in Fig. 3. First, the liquid meniscus is made protruding downward to form a convergent microlens; the hydrogel posts are in the expanded state (buffer *p*H=12.0), pushing against the substrate to bend the flexible aperture slip up. To mimic a changing *p*H environment, two syringe pumps are used to pump the new buffer into and suck the old buffer out of the chamber, respectively; their flow rates are set the same (0.4 ml/min) to alleviate the fluctuation of the water-oil interface. At low *p*H, the hydrogel posts contract and the aperture slip bends downward compared to the starting state, causing the microlens to bulge upward. When a *p*H-8.0 buffer is replaced with a *p*H-6.0 one, the microlens has a flat water-oil interface (infinite curvature) and transits from convergent to a divergent.

To determine the focal length of the microlens, the device is illuminated with a collimated laser beam (670 nm) from one side. Light passing through the microlens is collected by a microscope coupled to a charge-coupled device (CCD) camera. We first focus the microscope at the top-side surface of the aperture and then move the sample stage so that the microscope focuses to the image produced by the microlens. The distance that the stage travels is thus the distance between the microlens and its image, which, in turn, is the focal length of the microlens. Figure 4(a) shows a typical focal length of a microlens with different *p*H buffers. The focal length can be varied from -7.6 mm to $-\infty$ (divergent)

RIGHTSLINK

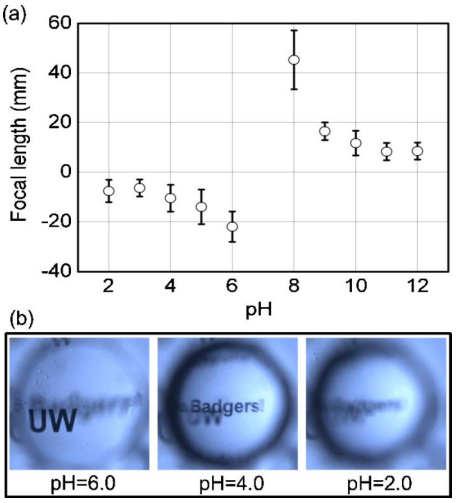

FIG. 4. (Color online) Tuning and focusing of the liquid microlens. (a) Focal length of liquid microlens as a function of the *p*H value. The transition of the microlens from divergent to convergent occurs between *p*H 6.0 and 8.0. (b) Output images of the printed "UW" and "Badgers!" on two transparencies through the microlens. UW and Badgers! are focused at *p*H 6.0 and *p*H 4.0, respectively. The focal point falls beyond both objects at *p*H 2.0.

and from 8.5 mm to $+\infty$ (convergent). The transition point (*p*H=6.0–8.0) can be adjusted by varying the starting shape of microlens, which allows to facilitate the design of the microlens for specific applications. The response time is observed to be around 10 s, taken from exposing the hydrogel to the desired *p*H buffers to a visual change of the shape of the microlens.

To evaluate the microlens's ability of variable focusing on objects at different distances, we print "UW" and "Badgers!" on two transparent films and position them 9 mm apart. The microlens is located above the films. Figure 4(b) shows the resulting output images through the microlens, observed through a stereoscope coupled to a CCD camera. The experiment starts with *p*H 6.0, at which UW is focused. When *p*H changes to 4.0, the microlens adjusts its focal length and focuses to Badger!. Both objects are out of focus at *p*H 2.0. The microlens in this test is divergent.

We also estimate the chromatic and spherical aberrations inherent to the liquid microlens. As the wavelength of light changes from 400 to 700 nm, the refractive indices of the mineral oil and water vary approximately from 1.48 to 1.46 and from 1.34 to 1.33, respectively. This causes a variation of 6.2% in the focal length across the visible spectrum range. To estimate the spherical aberration of the microlens, we fit the curves from the lens profiles using six order polynomials and calculate the Seidel spherical aberration coefficient using an optical simulation software, OSLO-LT6.1 (Sinclair Optics). The obtained Seidel spherical aberration coefficients for the microlenses at *p*H 2.0 and 6.0 are −0.074 and −0.092, respectively. Since each liquid microlens presented here essentially is a doublet lens made up of a divergent lens and a convergent lens with different optical properties of the lens materials (e.g., refractive index and chromatic dispersion), the chromatic and spherical aberrations can be minimized by tuning these optical properties[6] without the need for any additional lenses or postprocessing for imaging correction.

In summary, we have demonstrated liquid microlenses self-adaptive to environmental *p*H by combining hydrogels and pinned liquid-liquid interfaces. The microlenses have a wide range of adjustable focal lengths. Since diffusion becomes a significant mechanism of transport in hydrogels at the microscale,[14] scaling down the hydrogel structures allows faster response of the microlens. Compared to our previously reported scheme,[12] the implementation realized here may be more conducive to miniaturization for faster response: by patterning multiple small hydrogel posts, rather than a single thin hydrogel ring, larger area of hydrogel is exposed to the stimuli, and the mechanical robustness of the hydrogel structures is better. The self-adaptive behavior of the liquid microlens may prove beneficial in many optical sensing and imaging applications, since the self-adaptive functionality can further be extended to other environmental stimuli such as light, temperature, electric fields, and biological/chemical events. Such functionality for externally controlled systems might be difficult. For instance, sensing biological/chemical agents on a microchip itself can be quite challenging—most biological assays work on molecular binding events, which are then read out using complicated systems (e.g., optical, surface plasmon resonance, and spectroscopy). Our approach utilizes stimuli-responsive hydrogels to realize the sensing, thus bypassing the need for complicated detection systems, external control systems, and power supplies. Packaging of the microlenses will be further studied in the future.

This work is partly supported by the U.S. Department of Homeland Security (Grant No. N-00014-04-1-0659) through a grant awarded to the National Center for Food Protection and Defense at the University of Minnesota and is partly supported by the Wisconsin Alumni Research Foundation. The authors cordially thank David J. Beebe (University of Wisconsin-Madison) and his research group for fruitful discussion and access to their facilities. Discussion with Leon McCaughan, Abhishek K. Agarwal and Sudheer S. Sridharamurthy is also greatly appreciated.

[1] M. A. Burns, B. N. Johnson, S. N. Brahmasandra, K. Handique, J. R. Webster, M. Krishnan, T. S. Sammarco, P. M. Man, D. Jones, D. Heldsinger, C. H. Mastrangelo, and D. T. Burke, Science **282**, 484 (1998).
[2] S. Camou, H. Fujita, and T. Fujii, Lab Chip **3**, 40 (2003).
[3] K. Carlson, M. Chidley, K. B. Sung, M. Descour, A. Gillenwater, M. Follen, and R. Richards-Kortum, Appl. Opt. **44**, 1792 (2005).
[4] N. Chronis, G. L. Liu, K. H. Jeong, and L. P. Lee, Opt. Express **11**, 2370 (2003).
[5] S. Yang, T. N. Krupenkin, P. Mach, and E. A. Chandross, Adv. Mater. (Weinheim, Ger.) **15**, 940 (2003).
[6] S. Kuiper and B. H. W. Hendriks, Appl. Phys. Lett. **85**, 1128 (2004).
[7] H. W. Ren, Y. H. Fan, and S. T. Wu, Opt. Lett. **29**, 1608 (2004).
[8] H. W. Ren and S. T. Wu, Appl. Phys. Lett. **86**, 211107 (2005).
[9] D. Y. Zhang, V. Lien, Y. Berdichevsky, J. Choi, and Y. H. Lo, Appl. Phys. Lett. **82**, 3171 (2003).
[10] C. A. Lopez, C. C. Lee, and A. H. Hirsa, Appl. Phys. Lett. **87**, 134102 (2005).
[11] J. Kim, N. Singh, and L. A. Lyon, Angew. Chem., Int. Ed. **45**, 1446 (2006).
[12] L. Dong, A. K. Agarwal, D. J. Beebe, and H. Jiang, Nature (London) **442**, 551 (2006).
[13] L. Dong, A. K. Agarwal, D. J. Beebe, and H. Jiang, Adv. Mater. (Weinheim, Ger.) (in press).
[14] Y. Osada, J. P. Gong, and Y. Tanaka, J. Macromolecular Science-Polymer Reviews **C44**, 87 (2004).
[15] J. Atencia and D. J. Beebe, Nature (London) **437**, 648 (2005).
[16] The *p*H-sensitive hydrogel prepolymer mixture consists of acrylic acid, 2-hydroxyethyl methacrylate (0–50 ppm monomethyl ether hydroquinone inhibitor), ethylene glycol dimethacrylate, and 2,2-dimethoxy-2-phenylacetophenone in the weight ratio of 4.054:29.286:0.334:1.0.
[17] D. J. Beebe, J. S. Moore, Q. Yu, R. H. Liu, M. L. Kraft, B. H. Jo, and C. Devadoss, Proc. Natl. Acad. Sci. U.S.A. **97**, 13488 (2000).

RIGHTSLINK